Nuclear Physics A424 (1984) 221–238

THE PROMETHIUM ISOTOPES IN THE INTERACTING BOSON-FERMION MODEL

O. SCHOLTEN and T. OZZELLO

Cyclotron Laboratory and Department of Physics and Astronomy, Michigan State University, East Lansing, MI 48824, USA

Received 6 December 1983
(Revised 27 February 1984)

Abstract: We present a calculation of excitation energies, electromagnetic moments and transition rates and single-particle transfer amplitudes for the odd-mass promethium isotopes in terms of the interacting boson-fermion model. Model parameters are compared with those obtained for the neighbouring europium isotopes.

1. Introduction

In the interacting boson model (IBA) even-even nuclei are described as a system of interacting s- and d-bosons [1-3]. The IBA model distinguishes itself from most other boson models by the fact that in it the total number of bosons is strictly conserved for a given nucleus, which takes into account finite particle effects [4-6]. The conservation of boson number has some important consequences: from a calculational point of view it allows one to work with small finite matrices, from a microscopic point of view it allows for the interpretation of a boson as a collective fermion pair state [4]) and, most important, phenomenologically it allows for the description of spherical [1]), deformed [2,3]) and transitional [7,8]) nuclei using a single hamiltonian. The model has proven in many applications to give an accurate description of the properties of low-lying collective states in even-even nuclei [9]).

The IBA model has been extended to cover also odd-mass nuclei by coupling explicitly the degrees of freedom of the odd particle to the system of bosons [10,11]). This model, the interacting boson-fermion approximation (IBFA), has been applied to a few odd-mass isotopes [12]). The main incentive for the present investigation of the Pm ($Z = 61$) isotopes in the IBFA model is to obtain the parameters not only for a series of isotopes, but, in combination with the previous calculation for Eu ($Z = 63$) [ref. [13])], for a region in the periodic table.

In the following section the IBFA model is briefly outlined. After this, in sect. 3, the results of an IBA calculation for the Nd isotopes are presented, together with the

calculated excitation energies for the Pm isotopes. The Nd isotopes ($Z = 60$) serve as the core to which the odd proton is coupled. Calculated electromagnetic properties and single-particle transfer amplitudes for Pm isotopes are discussed in sects. 4 and 5. The obtained parameters are compared with those of Eu and the results of a simple microscopic calculation in sect. 6.

2. The model

In this section only a short overview of the IBFA model will be given. A more extensive description can be found in refs. [13, 14]). In the IBFA model odd-A nuclei are described by coupling the degrees of freedom of the odd particle to those of the bosons in the core. The hamiltonian can therefore be written in general as

$$H = H_B + H_F + V_{BF}, \tag{2.1}$$

where H_B is the pure boson part of the hamiltonian, describing the core. Since only a single odd particle is considered, the pure fermion part H_F of eq. (2.1) contains only one-body terms,

$$H_F = \sum_{jm} \varepsilon_j a^\dagger_{jm} a_{jm}, \tag{2.2}$$

where $a^\dagger_{jm}(a_{jm})$ is an odd-nucleon creation (annihilation) operator and ε_j are the quasiparticle energies. The structure of the solution is, however, determined by the boson-fermion interaction V_{BF}. The general two-body interaction contains prohibitively many free parameters and for this reason we will limit ourselves to the boson-fermion interaction that is suggested by microscopic calculations [13-15]),

$$V_{BF} = \sum_j A_j \hat{n}_d \hat{n}_j + \sum_{jj'} \Gamma_{jj'} (Q_B^{(2)} \cdot (a^\dagger_j \tilde{a}_{j'})^2) + \sum_{jj'j''} \Lambda^{j''}_{jj'} : ((d^\dagger \tilde{a}_j)^{(j'')} \times (\tilde{d} a^\dagger_{j'})^{(j'')})^{(0)}_0 :, \tag{2.3}$$

where

$$Q_B^{(2)} = (s^\dagger \tilde{d} + d^\dagger s)^{(2)} + \chi (d^\dagger \tilde{d})^{(2)}. \tag{2.4}$$

The first term in eq. (2.3) is a monopole-monopole interaction. This interaction is normally weak and does not influence the structure of the spectrum. Its main effect is to increase the d-boson energy. The second term, the quadrupole interaction, originates from the strong quadrupole component in the interaction between the odd proton and the neutron bosons. The last term, the exchange force, finds its origin completely in the Pauli principle; it takes into account that the bosons themselves are built up out of fermions which can occupy the same orbits as the odd particle.

In order to reduce the number of parameters we will assume for $\Gamma_{jj'}$ and $\Lambda^{j''}_{jj'}$ a j-dependence that is suggested by microscopic calculations:

$$\Gamma_{jj'} = \Gamma_0(u_j u_{j'} - v_j v_{j'})Q_{jj'},$$
$$\Lambda^{j''}_{jj'} = -2\sqrt{5}\Lambda_0 \beta_{jj''}\beta_{j''j'}/\sqrt{2j''+1}, \tag{2.5}$$

where

$$\beta_{jj'} = (u_j v_{j'} + v_j u_{j'})Q_{jj'},$$
$$u_j^2 = 1 - v_j^2. \tag{2.6}$$

The coefficients v_j^2 are related to the occupancy of the orbit j, and $Q_{jj'}$ are the single-particle matrix elements of the quadrupole operator. The dependence of the strength of the quadrupole force $\Gamma_{jj'}$ on the occupation probability is also a manifestation of the Pauli principle. It will be clear from eqs. (2.5) and (2.6) that in the case of a unique parity orbit, the $h_{\frac{11}{2}}$ in our case, there are only two linearly independent parameters.

In the evaluation of the single-particle matrix elements of the quadrupole operator all the radial integrals have been taken equal and thus

$$Q_{jj'} = \langle l\tfrac{1}{2}j \| Y^{(2)} \| l\tfrac{1}{2}j' \rangle. \tag{2.7}$$

The relation between the IBFA model parameters and the shell-model nucleon-nucleon interaction will be outlined in sect. 4. In the calculations discussed in this paper the model parameters are considered as phenomenological parameters which are adjusted so as to give a best reproduction of the experimental data.

3. Excitation and binding energies

The Pm isotopes ($Z = 61$) are described in the IBFA model by coupling the degrees of freedom of the last odd particle to the Nd core ($Z = 60$). The Nd isotopes have been calculated before [11]) in the IBA II [16]) model, in a study that simultaneously included a description of the Nd, Sm and Gd isotopes. Since the IBFA calculations are based on the IBA-1 model, the parameters were projected from the IBA-2 model space onto that of the IBA-1 model [11]). It has been verified that the quality of the description of the Nd isotopes was unaffected by this procedure, and the calculated spectra for Nd are shown in fig. 1 while some B(E2) values are shown in fig. 2.

In the description of negative-parity states in Pm the odd particle is taken to be in the $h_{\frac{11}{2}}$ orbit while for the positive-parity states only the $d_{\frac{5}{2}}$ and $g_{\frac{7}{2}}$ orbits have been considered. In this latter case the $d_{\frac{3}{2}}$ and $s_{\frac{1}{2}}$ orbits can be neglected since, due

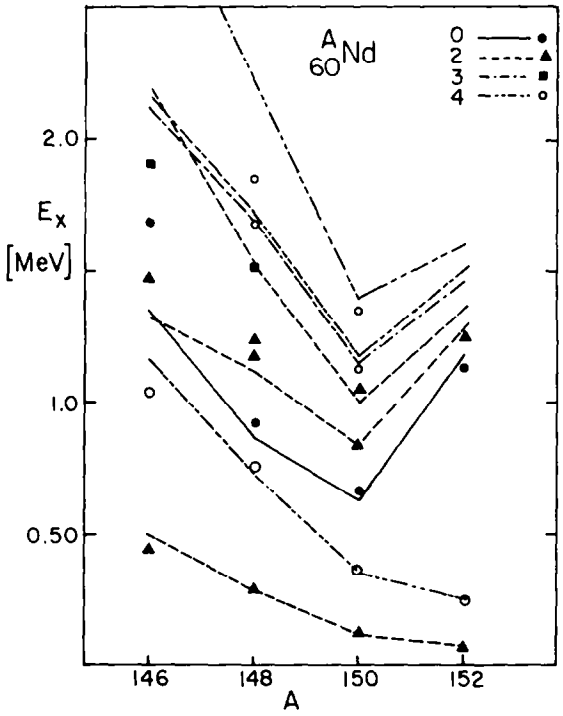

Fig. 1. Experimental[17]) and calculated[11]) excitation energies for the even-mass Nd isotopes.

to the gap in single-particle energies, the states built on these states lie much higher in the energy spectra and have therefore a small or negligible influence on the low-lying states.

The parameters describing the odd particle and the coupling of the odd particle to the bosons in the core (eqs. (2.3)–(2.6)) were obtained from a best fit to the experimental excitation energies in the Pm isotopes, while insisting on parameters that vary smoothly and systematically from isotope to isotope. The parameters are given in table 1. The strength of the monopole force has been taken equal to $A_j = -0.1$ MeV, constant for all nuclei and orbits. The calculation has been done using the program ODDA[18]).

In fig. 3 the calculated energies for positive-parity levels are compared with experiment. The spectrum of ^{147}Pm shows all the characteristics of a particle vibration spectrum[28]), the lowest lying $\frac{5}{2}^+$ and $\frac{7}{2}^+$ levels are the single-particle states while there occurs a multiplet of states at about the excitation energy of the 2_1^+ state in the core. In the heavier isotopes some well-developed rotational bands[29]) are present. The position of the $K = \frac{3}{2}^+$ band in ^{153}Pm depends strongly on the differences in occupancies for the $d_{\frac{3}{2}}$ and $g_{\frac{7}{2}}$ levels. If the occupancies are

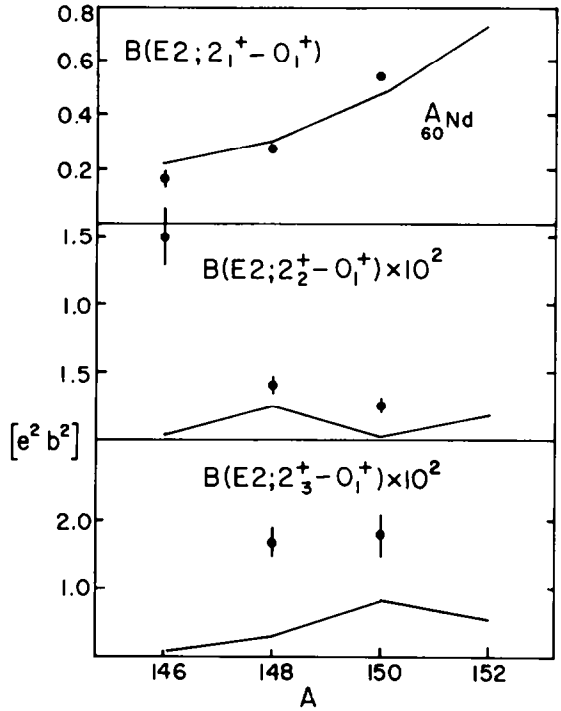

Fig. 2. Some experimental [19]) and calculated [11]) B(E2) values for the even-mass Nd isotopes.

taken equal, the $\frac{3}{2}^+_1$ level is calculated about 200 keV too low. In the calculations for the Eu isotopes [13]) the occupancies for the two s.p. levels could be kept equal since the $\frac{3}{2}^+_1$ level occurs at a lower excitation energy. In this respect ^{153}Pm is the first nucleus fitted in the IBFA model that shows the importance of different

TABLE 1

Values of the parameters as used in the calculation of the Pm isotopes (Γ_0 and Λ_0 are given in units of MeV)

N	86	88	90	92
Γ_0^+	0.485	0.63	0.75	0.82
Λ_0^+	0.65	0.84	1.00	1.09
$v^2_{d_{5/2}}$	0.64	0.55	0.46	0.405
$v^2_{g_{7/2}}$	0.64	0.59	0.54	0.52
$\varepsilon_{d_{5/2}} - \varepsilon_{g_{7/2}}$	0.1	0.25	0.45	0.75
Γ_0^-	0.94	1.26	1.52	1.67
Λ_0^-	2.52	3.39	4.11	4.51
$v^2_{h_{11/2}}$	0.18	0.255	0.33	0.33

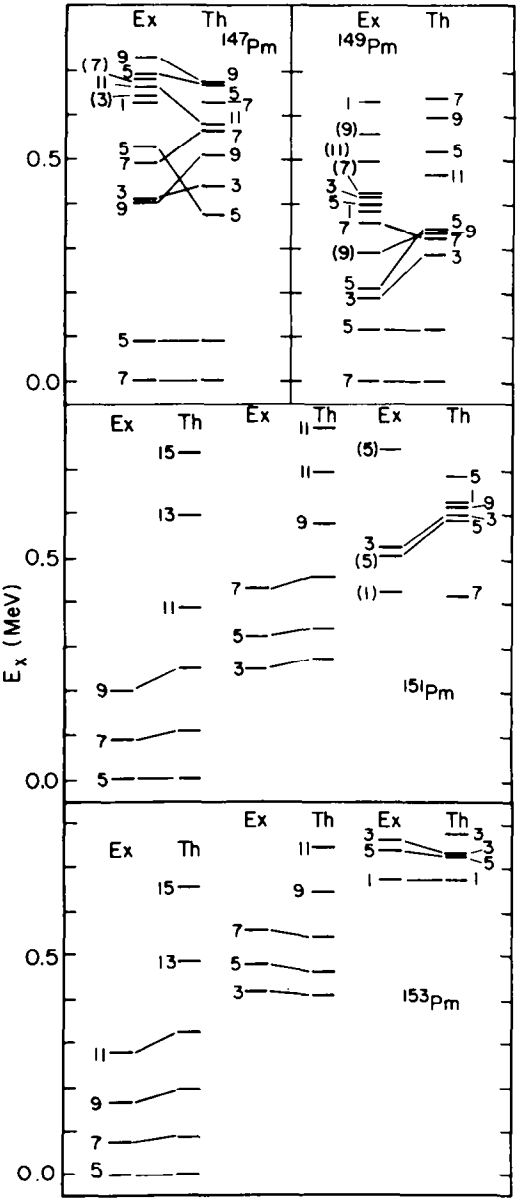

Fig. 3. Experimental[20-28]) and calculated relative energies of positive-parity levels for the odd-mass Pm isotopes. The levels are labelled with twice their spin value.

occupation probabilities already in the calculation of excitation energies. For the negative-parity levels a similar change in structure from spherical to deformed is observed. For ^{147}Pm a multiplet of levels is calculated at the excitation energy of

the 2_1^+ level in the core (see fig. 4). In experiment several levels have been observed in this energy region with uncertain spin (and sometimes even parity) assignments. There is, however, evidence that the calculated levels of the multiplet are too high

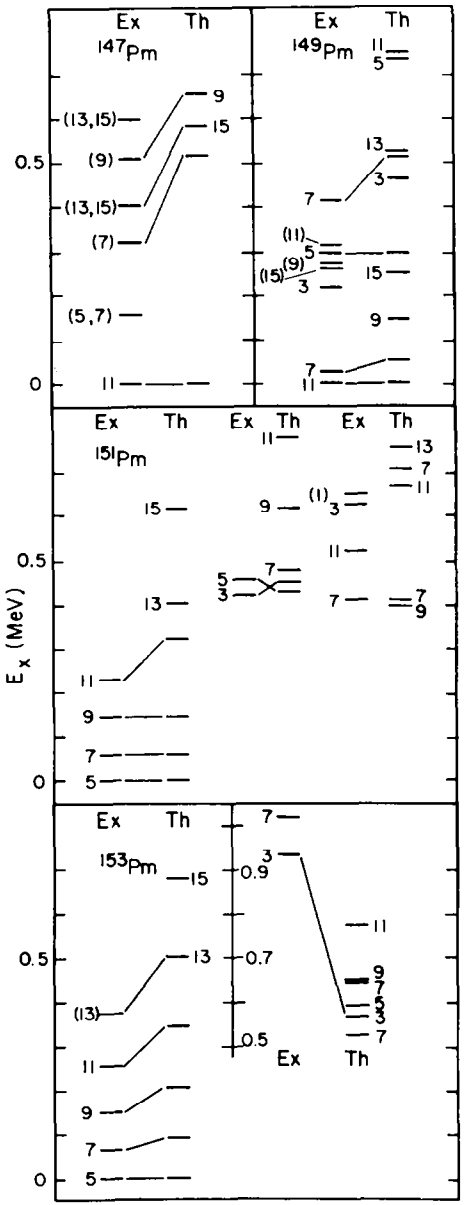

Fig. 4. Experimental[20-28]) and calculated relative energies of negative-parity levels for the odd-mass Pm isotopes. The levels are labelled with twice their spin value.

compared to experiment. This can be a result of the omission of the collective octupole degree of freedom from the calculation. In ^{147}Pm the excitation energy of the $\frac{11}{2}^-_1$ state is 0.649 MeV, while in the core nucleus ^{146}Nd the 3^-_1 state occurs at an excitation energy of 1.19 MeV. The position in the spectrum of the quintuplet resulting from the coupling $2^+ \times h_{\frac{11}{2}}$ is thus about the same as that of the multiplets arising from $3^- \times d_{\frac{5}{2}}$ and $3^- \times g_{\frac{7}{2}}$. The latter are, however, not considered in the present calculation. The mixing between these multiplets will bring certain levels down from their unperturbed position and this can account for the observed discrepancy between experiment and theory. In ^{149}Pm this effect is much less imporant since the $\frac{11}{2}^-_1$ level lies at an excitation energy of only 0.24 MeV while the 3^- in the core is at 1.0 MeV. In ^{153}Pm the position of the excited negative-parity bands is predicted too low. This points towards an underestimate of the strength of the boson-fermion interaction. The agreement with experiment cannot be improved by increasing the strengths of the quadrupole and the exchange forces since this will give rise to a too low value of the moment of inertia in the ground-state band. Again it could be the results of the omission of a collective octupole degree of freedom from the calculation which effectively can include additional terms in the boson-fermion interaction. On the basis of systematics [17]) one can expect the bandhead of a $K = 1^-$ band in ^{152}Nd at an excitation energy of only about 0.8 MeV.

4. Electromagnetic transition

In the IBFA model the electromagnetic transition operator is written as a sum of two terms,

$$T^{(\lambda)} = T_B^{(\lambda)} + T_F^{(\lambda)}, \tag{3.1}$$

where T_B^λ acts only on the boson part of the wave function and has the same form as in the IBA model, while T_F^λ acts only on the fermion part. In general one will have also mixed boson-fermion terms contributing to the transition operator, arising from the effects of the Pauli principle. In the present investigation we will limit ourselves, however, to the form given in eq. (3.1.).

4.1. E2 TRANSITIONS

In the IBA model the quadrupole transition operator is written as

$$T_B^{(2)} = e_B[(s^\dagger \tilde{d} + d^\dagger s)^{(2)} + \chi(d^\dagger \tilde{d})^{(2)}]. \tag{3.2}$$

The odd fermion contribution can be written as

$$T_F^{(2)} = e_F \sum_{jj'} Q_{jj'} (a_j^\dagger \tilde{a}_{j'})^{(2)}, \tag{3.3}$$

TABLE 2

Some calculated and measured B(E2) values (in units of $e^2 \cdot b^2$) for ^{149}Pm (the calculated $\frac{5}{2}^+_2$ level has been identified with the $\frac{5}{2}^+_1$ level and vice versa)

$\frac{5}{2}^+_1 \rightarrow \frac{7}{2}^+_1$	0.012 ± 0.003	0.0016
$\frac{3}{2}^+_1 \rightarrow \frac{7}{2}^+_1$	0.014 ± 0.002	0.024
$\frac{3}{2}^+_1 \rightarrow \frac{5}{2}^+_1$	0.32 ± 0.01	0.34
$\frac{5}{2}^+_2 \rightarrow \frac{7}{2}^+_1$	0.11 ± 0.01	0.17
$\frac{7}{2}^-_1 \rightarrow \frac{11}{2}^-_1$	0.56 ± 0.01	0.58

where $Q_{jj'}$ equals the single-particle matrix elements of the quadrupole operator (2.7). The boson effective charge was taken from a best fit to the Nd isotopes, $e_B = 0.139\ e \cdot b$ while the parameter χ has been taken equal to the SU(3) value, $\chi = -\frac{1}{2}\sqrt{7}$. The results of the calculation for Nd using these parameters was given in fig. 2. Microscopic calculations suggest that the fermion effective charge e_F is of the same order of magnitude as that of the bosons. For simplicity the two have therefore been taken equal, $e_F = e_B = 0.139\, e \cdot b$. In table 2 the calculated B(E2) values for ^{149}Pm are compared with experiment. In the table the experimental $\frac{5}{2}^+_1$ level is correlated with the calculated $\frac{5}{2}^+_2$ level and vice versa. The reason for this crossed relation is that experimental the $B(\mathrm{E2}; \frac{3}{2}^+_1 \rightarrow \frac{5}{2}^+_1)$ and $B(\mathrm{E2}, \frac{5}{2}^+_2 \rightarrow \frac{7}{2}^+_1)$ are relatively strong and so are $B(\mathrm{E2}; \frac{3}{2}^+_1 \rightarrow \frac{5}{2}^+_2)$ and $B(\mathrm{E2}; \frac{5}{2}^+_1 \rightarrow \frac{7}{2}^+_1)$ in the calculation. The B(E2) value connecting the $\frac{3}{2}^+_1$ and $\frac{5}{2}^+_1$ levels is of the same order of magnitude as the $B(\mathrm{E2}; 2^+_1 \rightarrow 0^+_1)$ in the core which signifies that the $\frac{3}{2}^+_1$ belongs to the multiplet obtained by coupling the $d_{\frac{5}{2}}$ s.p. degree of freedom to the 2^+_1 state of the core. The other members of this multiplet are the calculated $\frac{1}{2}^+_1$, $\frac{5}{2}^+_3$, $\frac{7}{2}^+_3$ and $\frac{9}{2}^+_2$ levels. The $\frac{5}{2}^+_2$ level has been pushed down by the influence of the Pauli principle. In the calculation this is taken into account via the exchange force.

A calculation of quadrupole moments is presented in fig. 5. Large changes are predicted especially in $Q_{\frac{7}{2}^+_1}$. The change arises from the fact that for the lighter isotopes the $\frac{7}{2}^+_1$ state is a rather pure $g_{\frac{7}{2}}$ s.p. state while in the heavier isotopes it belongs to a $K = \frac{5}{2}^+$ band.

4.2. M1 TRANSITIONS

In the IBA model the lowest-order M1 operator,

$$T^{(1)}_B = g_d (d^\dagger \tilde{d})^{(1)} \sqrt{30/4\pi}, \tag{3.4}$$

does not give rise to M1 transitions since it is proportional to the angular momentum operator. In order to be able to calculate M1 transitions in even-even nuclei, terms which are higher order in the boson operators have to be included.

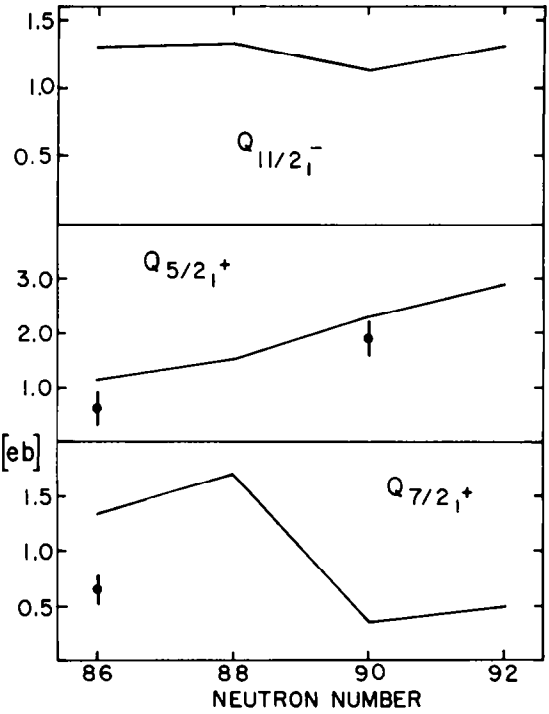

Fig. 5. Some experimental[30]) and calculated values of quadrupole moments.

The operator eq. (3.4) does account for a d-boson g-factor. For odd nuclei this operator can give a contribution to M1 transitions since the boson angular momentum is no longer a good quantum number. One should, however, expect to see the effect of the omission of higher-order terms in the boson operator, especially for weak transitions. For the strong M1 transitions and in the calculation of g-factors, however, the contribution of the odd-fermion is dominating,

$$T_{\mathrm{F}}^{(1)} = -\sum_{jj'} g_{jj'} \sqrt{j(j+1)(2j+1)/4\pi}\,(a_j^{\dagger}\tilde{a}_{j'})^{(1)},$$

$$g_{jj'} = \begin{cases} [(2j-1)g_l + g_s]/2j, & j = j' = l+\tfrac{1}{2} \\ [(2j+3)g_l - g_s]/2(j+1), & j = j' = l-\tfrac{1}{2} \\ (g_l - g_s)\sqrt{\dfrac{2l(l+1)}{j(j+1)(2j+1)(2l+1)}}, & j' = j-1, \end{cases} \tag{3.5}$$

where the orbital angular momenta of the two orbits j and j' have to be equal, $l = l'$; the last term therefore does not enter in the present description.

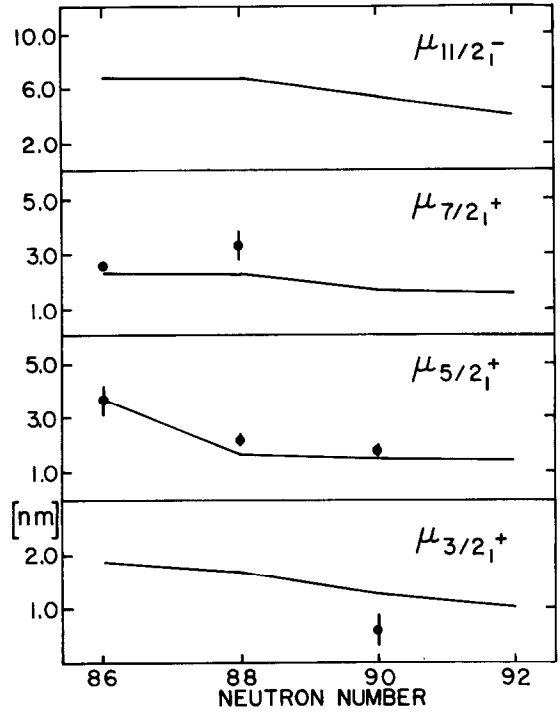

Fig. 6. Some experimental [30]) and calculated values of magnetic moments.

The boson g-factor g_d, has been extracted from the g-factors of the 2_1^+ state in the Nd isotopes giving $g_d = 0.25$ n.m. The s.p. estimates for g_l and g_s are $g_l = 1.0$ n.m. and $g_s = 5.585$ n.m. Quenching the g_s by factor ~ 0.7 to $g_s = 4.0$ n.m. improved the agreement between calculated and experimental magnetic moments considerably. This quenching is equal to what has been taken in the calculation of the Eu isotopes [13]) and in a shell-model calculation for the $N = 82$ isotones [32]).

The calculated magnetic moments are compared with experiment in fig. 6. In table 3 some calculated B(M1) are compared with the experimental values for

TABLE 3

Some calculated and experimental B(M1) values (in units of $10^{-2}\mu_N^2$) for ^{149}Pm

	Exp	Calc
$\frac{5}{2_1}^+ \rightarrow \frac{7}{2_1}^+$	0.48 ± 0.02	0.07
$\frac{3}{2_1}^+ \rightarrow \frac{5}{2_1}^+$	0.25 ± 0.04	1.05
$\frac{5}{2_2}^+ \rightarrow \frac{7}{2_1}^+$	3.6 ± 0.8	3.9
$\frac{5}{2_2}^+ \rightarrow \frac{5}{2_1}^+$	2.2 ± 0.4	2.5
$\frac{3}{2_1}^+ \rightarrow \frac{5}{2_2}^+$		0.63

^{149}Pm. Also here the calculated $\frac{5}{2_1}^+$ state is identified with the experimental $\frac{5}{2_2}^+$ state and vice versa.

5. Single-particle transfer

The operator for calculating single-particle (s.p.) transfer reactions connects even- and odd-mass nuclei and will therefore contain terms that are mixed in boson and fermion degrees of freedom. The operator can be written in general as a sum of two terms:

$$T_j^\dagger = A_j^\dagger + B_j^\dagger, \tag{5.1}$$

where the first term describes s.p. transfer where both the even and the odd nucleus have N bosons,

$$A_j^\dagger = \left[u_j a_j^\dagger - \sum_{j'} \frac{v_j}{\sqrt{N_\pi}} \sqrt{\frac{10}{2j+1}} \frac{N_\pi}{N} \beta_{j'j} (K_\beta)^{-1} s^\dagger (\tilde{d} a_{j'}^\dagger)^{(j)} \right] \Big/ K_j^a, \tag{5.2}$$

and the second term the case in which the odd nucleus has N and the even nucleus has $N+1$ bosons,

$$B_j^\dagger = \left[\frac{v_j}{N} (s^\dagger \tilde{a}_j)^{(j)} + \sum_{j'} u_j \sqrt{\frac{10}{2j+1}} \frac{N_\pi}{N} \beta_{j'j} (K_\beta)^{-1} (d^\dagger \tilde{a}_{j'})^{(j)} \right] \Big/ K_j^b, \tag{5.3}$$

with

$$K_\beta^2 = \sum \beta_{jj'}^2. \tag{5.4}$$

The specific forms eqs. (5.2)–(5.3) are suggested by a microscopic derivation of the IBFA model [11, 14]). The $(d^\dagger a_{j'}^\dagger)^{(j)}$ s-term, for example, is not included in eq. (5.2) even though it is of the same order as the other terms. According to the microscopic picture [11, 14]) this would correspond to a term changing the seniority by 3 in the fermion space which, of course, is not allowed for a single-particle operator. The coefficients u_j, v_j and $\beta_{jj'}$ have been taken equal to those that enter in the hamiltonian, eqs. (2.5), (2.6). In the microscopic derivation, eqs. (5.2), (5.3) represent a lowest-order approximation to the full operator and for this reason violate sum rules. In order to preserve these, renormalization factors K_j^a and K_j^b have been introduced. These factors are determined by the conditions

$$\sum_{\text{odd}} \langle \text{odd} | A_j^\dagger | \text{even} \rangle^2 = (2j+1) u_j^2,$$

$$\sum_{\text{odd}} \langle \text{even} | B_j^\dagger | \text{odd} \rangle^2 = (2j+1) v_j^2.$$

In a more phenomenological treatment of s.p. transfer one could consider independent normalization for each of the two terms in both eqs. (5.3) and (5.4).

In figs. 7, 8 and 9 the calculated spectroscopic factors for the two lowest-lying $\frac{5}{2}^+$, $\frac{7}{2}^+$ and $\frac{11}{2}^-$ levels are compared with experiment. The general trend is that the spectroscopic factor to the lowest state decreases with increasing mass. This trend is easily understood in a weak-coupling picture, since with increasing deformation the coupling strength of the odd-particle to the core will increase. This will give rise to a distribution of the s.p. transfer strength over more levels and thus decrease the strength to the first level which is almost a pure s.p. state in ^{147}Pm. More quantitative statements are difficult to make since there is a large scatter in the experimental data. The fact, however, that the $d_{\frac{5}{2}}$ spectroscopic factor to the $\frac{5}{2}^+_1$ level in ^{151}Pm and ^{153}Pm drops essentially to zero can be understood in a pseudo-spin picture [33]). Together with the $\frac{3}{2}^+_1$ level, the $\frac{5}{2}^+_1$ level belongs to a pseudo $l = 2$ multiplet which has a zero spectroscopic factor since the coupled odd particles form a pseudo-($l = 3$) multiplet.

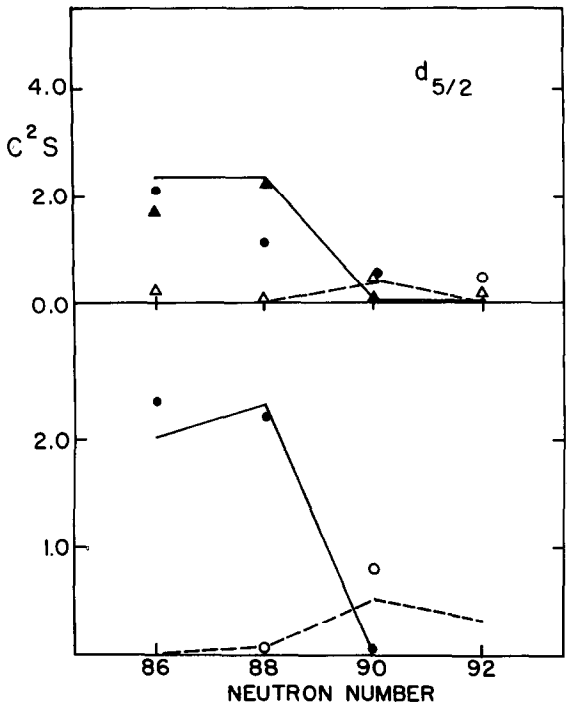

Fig. 7. Measured and calculated spectroscopic factors for $d_{5/2}$ transfer. The upper (lower) part of the figure shows results for the pickup (stripping) reaction leading to Pm. Closed and open circles represent the data of the (d, ^{3}He) [ref. [28])] and (^{3}He, d) [refs. [24, 25])] reactions leading to the first respectively second $\frac{5}{2}^+$ states. The closed and open triangles represent the corresponding data for the (t, α) [refs. [24–27])] reactions. The solid and dashed lines show the results of the calculation.

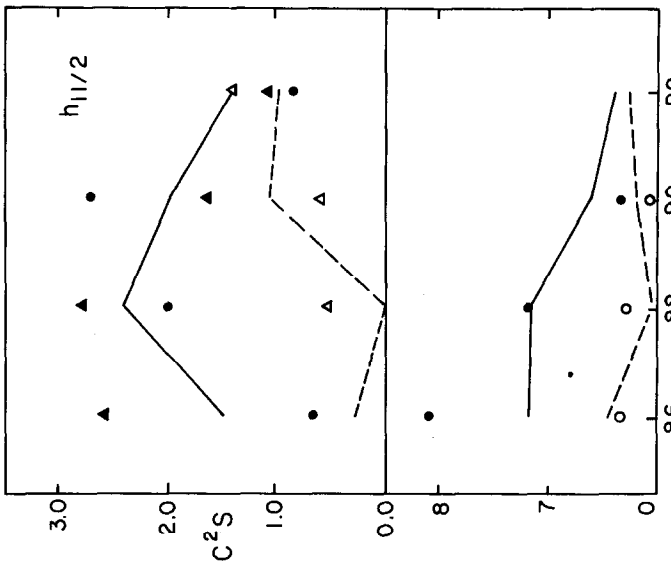

Fig. 9. Same as fig. 7 but for $h_{11/2}$ transfer leading to $\frac{11}{2}^-$ states.

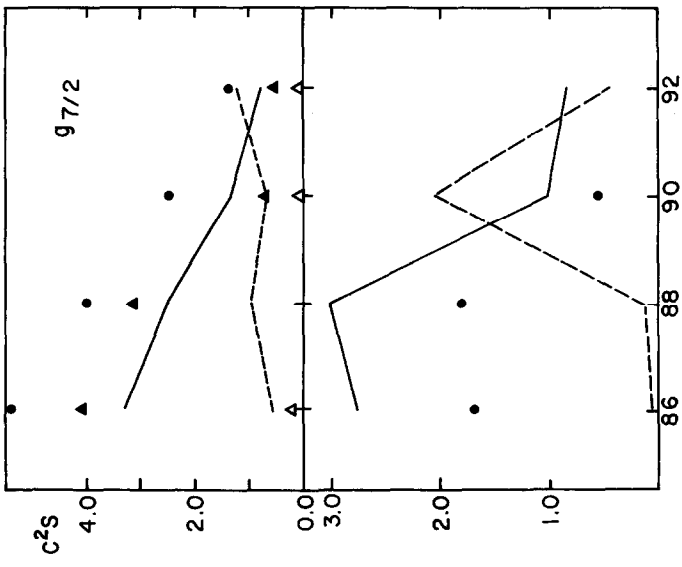

Fig. 8. Same as fig. 7 but for $g_{7/2}$ transfer leading to $\frac{7}{2}^+$ states.

6. Microscopic analysis of the parameters

As was mentioned in sect. 2, the parameters Γ_0, Λ_0 and v^2 cannot be determined unambiguously from a χ^2 fit since they are linearly dependent. In principle one would expect to obtain the same values for Γ_0 and Λ_0 for both positive- and negative-parity states. In the calculation of the s.p. matrix elements of the quadrupole operator all radial matrix elements have been taken equal. When comparing positive- and negative-parity states this might not be a good approximation. Since the radial integrals enter linearly in the calculation of the quadrupole force and quadratically in the exchange force we have instead kept Γ_0^2/Λ_0 the same for positive- and negative-parity states. Another condition that has been imposed to reduce the number of parameters is that the ratio $R = \Gamma_0/\Lambda_0$ is constant as a function of N for both positive- and negative-parity states. This condition does not follow from a microscopic theory, but has been imposed since it is easier to use than the condition $\sum_j v_j^2(2j+1) = 11$. Furthermore in the calculation for the Eu isotopes this assumption happened to agree with the microscopic calculations. It can be verified from table 1 that indeed $\sum_j v^2(2j+1) \approx 11$, the number of protons in a valence shell.

A microscopic derivation of the boson-fermion interaction gives

$$\Gamma_0 = \bar{\kappa} N_\nu/(N_\nu + N_\pi), \tag{6.1}$$

$$\Lambda_0 = \bar{\kappa} \frac{1}{K_\beta} N_\nu \sqrt{10 N_\pi}/(N_\nu + N_\pi), \tag{6.2}$$

$$\kappa = -\bar{\kappa} K_\beta / \sqrt{2 N_\pi}, \tag{6.3}$$

where β is defined by eq. (2.6) and K_β by eq. (5.4). In the derivation it has been assumed that the origin of the boson-fermion interaction lies in the neutron-proton quadrupole force with a strength proportional to κ. The fact that in the IBFA code no distinction is being made between neutron and proton degrees of freedom introduces the explicit N-dependence in eqs. (6.1)–(6.3). In fig. 10 the values obtained for Γ_0 and v_j^2 are plotted for both the Pm and Eu isotopes. The large difference between the extracted values of Γ_0 for positive and negative parity is not well understood. Only a small part of this can be explained by the difference in the radial integrals. Part of it could also come from the fact that the interaction between valence neutrons and the $h_{\frac{11}{2}}$ proton orbit is much larger than that between the neutrons and the positive-parity orbits. Furthermore the importance of the collective octupole degree of freedom in the calculation should be investigated.

The value for the ratio $R = \Gamma_0/\Lambda_0$, calculated from eqs. (6.1), (6.2), ranges from 0.2 for ^{147}Pm to 0.22 for ^{153}Pm. The assumption that R is a constant for all

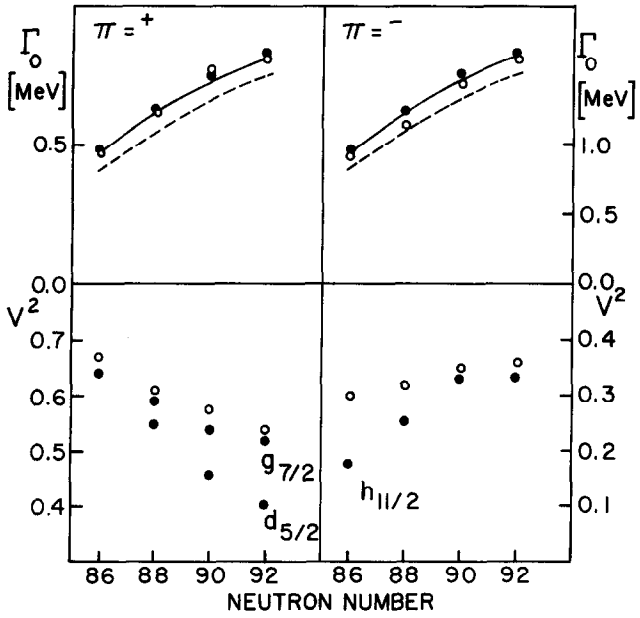

Fig. 10. Comparison of the present IBFA model parameters (closed circles) and those obtained from a calculation on the Eu isotopes (open circles). The curves give the expected N- and Z-dependence of the parameters (solid: Pm, dashed: Eu).

isotopes turned out to be well justified. The numerical value of this ratio is however much smaller than what has been obtained for either negative- ($R = 0.37$) or positive-parity ($R = 0.75$) states. The reason for this difference is unclear but could lie in the fact that part of the particle-boson interaction finds its origin in the interaction between like nucleons [34]).

7. Summary

In this paper IBFA calculations for the odd-mass Pm isotopes have been presented. The results of phenomenological calculations have been compared with the data. The transition from a spectrum typical of a particle-core weak-coupling scheme to that of the Nilsson scheme is correctly reproduced. In general a good quantitative agreement between calculation and experiment is obtained. One of the largest discrepancies is found in the spectrum of ^{153}Pm where the excited negative-parity band is predicted about 300 keV too low.

The model parameters as obtained from the present calculations are very similar, as well as in magnitude as in the N-dependence, to those obtained in a previous calculation for the Eu isotopes. There is also a qualitative agreement with the

predictions of a simple microscopic theory. The fact that the ratio of the strength of the exchange and the quadrupole force is different from the value predicted by the above microscopic theory, which relates both forces to the neutron-proton quadrupole force, might be an indication that there is a large contribution to the exchange force coming from the interaction between like particles as was suggested in ref. [34]). This investigation also has shown that a more detailed understanding of the importance of the octupole degree of freedom in the calculation is required.

I wish to thank W. B. Walters for many interesting discussions and a critical review of the experimental data. Thanks are also due to J. Wood. This work was supported by the National Science Foundation under grant no. PHY-80-17605.

References

1) A. Arima and F. Iachello, Ann. of Phys. **99** (1976) 253
2) A. Arima and F. Iachello, Ann. of Phys. **111** (1979) 201
3) A. Arima and F. Iachello, Ann. of Phys. **123** (1979) 468
4) A. Arima, T. Otsuka, F. Iachello and I. Talmi, Phys. Lett. **66B** (1977) 205
5) T. Otsuka, A. Arima and F. Iachello, Nucl. Phys. **A309** (1978) 1
6) T. Otsuka, Ph.D. thesis, University of Tokyo (1979)
7) O. Scholten, F. Iachello and A. Arima, Ann. of Phys. **115** (1979) 325
8) R. F. Casten and J. A. Cizewski, Nucl. Phys. **A309** (1978) 477
9) See e.g. Interacting bosons in nuclear physics, ed. F. Iachello (Plenum, New York, 1979)
10) F. Iachello and O. Scholten, Phys. Rev. Lett. **43** (1979) 679
11) O. Scholten, Ph.D. thesis, University of Groningen, The Netherlands (1980)
12) F. Iachello, in Interacting Bose-Fermi systems in nuclei, ed. F. Iachello (Plenum, New York, 1981) p. 273;
O. Scholten, *ibid.*, p. 285;
P. von Brentano, A. Gelberg and U. Kaup, *ibid.*, p. 303;
R. F. Casten, *ibid.*, p. 317
J. Wood in Contemporary research in nuclear physics, ed. D. H. Feng *et al.* (Plenum, New York, 1981) p. 451;
O. Scholten, *ibid.*, p. 503
13) O. Scholten and N. Blasi, Nucl. Phys. **A380** (1982) 509
14) O. Scholten and A. E. L. Dieperink, in Interacting Bose-Fermi systems in nuclei, ed. F. Iachello (Plenum, New York, 1981) p. 328
15) I. Talmi, in Interacting Bose-Fermi systems in nuclei, ed. F. Iachello (Plenum, New York, 1981) p. 329
16) T. Otsuka, A. Arima, F. Iachello and I. Talmi, Phys. Lett. **76B** (1978) 139
17) M. Sakai, Quasi-bands, Inst. for Nuclear Study, Univ. of Tokyo (1982)
18) O. Scholten, program package "ODDA", KVI internal report no. 255 (1980)
19) A. Bäcklin, private communication
20) B. Harmatz and W. B. Ewbank, Nucl. Data Sheets **25** (1978) 113;
M. A. Lee, Nucl. Data Sheets **37** (1982) 303
21) R. B. Begzhanov, K. Sh. Azimov, S. Kh. Salimov and K. T. Teshabaev, Sov. J. Phys. **23** (1976) 3
22) W. B. Walters, M. D. Glascock, E. W. Schneider, R. A. Meyer, H. A. Smith, Jr. and M. E. Bunker, Inst. Phys. Conf. Ser. **51** (1980) 303
23) E. W. Schneider, M. D. Glascock, W. B. Walters and R. A. Meyer, Z. Phys. **A291** (1979) 77;
W. B. Walters, private commucation
24) O. Straume, G. Løvhøiden and D. G. Burke, Z. Phys. **A290** (1979) 67

25) O. Straume, G. Løvhøiden, D. G. Burke, E. R. Flynn and J. W. Sunier, Nucl. Phys. **A322** (1979) 13
26) O. Straume, G. Løvhøiden, D. G. Burke, E. R. Flynn and J. W. Sunier, Z. Phys. **A293** (1979) 75
27) D. G. Burke, G. Løvhøiden, E. R. Flynn and J. W. Sunier, Phys. Rev. **C18** (1978) 693
28) I. S. Lee, W. J. Jordan, J. V. Maher, R. Kamermans, J. W. Smits and R. H. Siemssen, Nucl. Phys. **A371** (1981) 111
29) See e.g. A. Bohr and B. R. Mottelson, Nuclear structure, vol. II (Benjamin, Reading, Mass., 1975)
30) V. S. Shirley and C. M. Lederer, Table of isotopes (Lawrence Berkeley Lab., 1979)
31) P. M. Endt, Atom. Nucl. Data Tables **26** (1981) 48
32) H. Kruse, private communication
33) O. Scholten, Phys. Lett. **108B** (1982) 155
34) A. Gelberg, private communication